# The effect of Weber number and spread factor of a water droplet impinging on a super-hydrophobic substrate

Darin Comeau, Kevin LaTourette, and John Pate

December 3, 2007

Program in Applied Mathematics, University of Arizona
Tucson, AZ USA 85721

**Abstract**

This paper uses experimental data to analyze how the Weber number ($We$) and spread factor ($\beta$) of a water droplet impinging on a super-hydrophobic substrate are related to the droplet's behavior during impact and subsequent primary rebound. We analyze the dissipation of energy prior to impact theoretically, and derive a non-dimensional system of differential equations to model the dynamics. A critical We value of 100 is provided which is a predictor for water droplet splashing for our substrate. We also confirm the Ohnesorge number of water droplets in the We range of 30-150 to be $\approx 1.8 \times 10^{-3}$ using our experimental data.

# 1 Introduction

Collisions of liquid droplets with solid surfaces are observed in everyday scenarios, from raindrops falling on a windshield, pouring the morning coffee, or watering one's lawn. Understanding the processes that affect impact behavior is extremely useful to a wide variety of applications. When spraying herbicides and pesticides in the agricultural industry, it is best to have the liquid stick to the plant surfaces to increase the effectiveness of the spray and decrease contamination of the soil [1]. In other situations, it is ideal for water to be repelled from surfaces, including windshields, clothes, and roofs. Understanding droplet impact behavior can also be applied to paints, ink jet printers, and household cleaners for example. In all of these cases, we have a low viscous fluid coming into contact with a smooth surface. Thus the information gathered from our research is general and the methods can be applied to multiple applications.

Our experiment studies the motion of a water droplet as it impinges on a glass slide coated with a super-hydrophobic treatment[1], and the response of the droplet immediately

[1]Substrate used was a glass slide first covered in soot, then coated with Kiwi shoe protector.

following impact. The substrate is oriented perpendicular to the fall of the droplet, directly below the path of the droplet. Our data analysis then focuses on the initial fall, the spreading of the droplet upon impact, and the first rebound bounce. The same substrate and fluid is maintained throughout the experiment; the only variable being the initial height of the droplet.

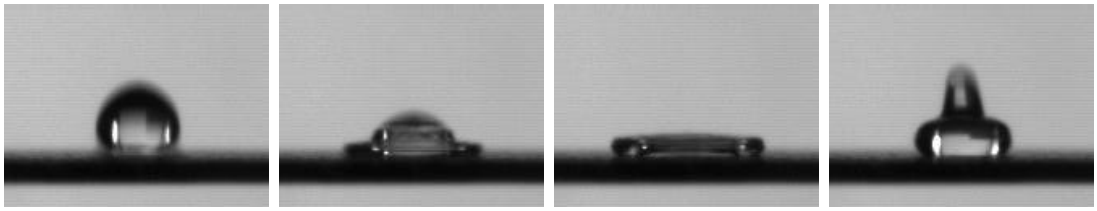

Figure 1: Water droplet impinging on surface dropped from a height of 33mm. The third frame displays maximum droplet spreading into a pancake shape, followed by the formation of the Worthington jet.

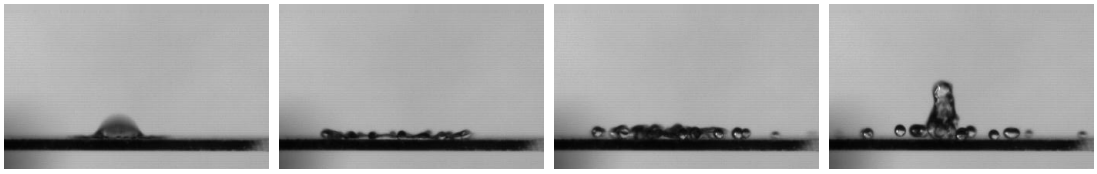

Figure 2: Water droplet impinging on surface dropped from a height of 145mm. The second frame displays maximum spreading with finger formation prior to splashing. The third frame displays droplet splash behavior, followed by rebound motion.

The dynamics at impact is driven by an interplay between the kinetic energy and the surface tension of the droplet. There are two typical behaviors observed upon impact - spreading and splashing. In both cases, the water droplet initially flattens and spreads out horizontally into a pancake shape. The Weber number of a spherical fluid is defined to be the dimensionless quantity

$$\mathrm{We} = \frac{\rho v^2 D_0}{\gamma}$$

where $\rho$ is the fluid density, $v$ is the droplet velocity at impact, $D_0$ is the droplet diameter, and $\gamma$ is the surface tension. For small We, the surface tension of water is strong enough to stop the spreading which can be seen in Figure 1. For larger We, the kinetic energy of the water spreading is greater than the surface tension. Water then groups into fingers along the outer rim of the droplet which have sufficient energy to overcome the surface tension and pinch off into smaller droplets. After the initial spreading/splashing, the surface tension pulls inward creating an upward flow of water known as a Worthington Jet, as we see in image 4 of Figure 1 and Figure 2.

In this paper we determine how the We of a water droplet before impact, and the droplet's spread factor $\beta = d/D_0$, where $d$ is the maximum spreading diameter upon impact, affects

the rebound height and cohesive properties of the droplet after impact. Furthermore, we study the dissipation of energy from the water droplet during the experiment both internally through viscous dissipation and externally due to the drag force of the moving droplet. We also present a phase portrait of the nondimensionalized system, and a critical We above which splashing will occur.

Water impinging a solid substrate is a fundamental problem that has been the topic of numerous research papers. The impact is very complex, and thus has not been thoroughly explained. For low We $\sim$ 1.42, Foote [3] accurately modeled the dynamics of impact by numerical integration of the Navier-Stokes equations. Sikalo et. al. [7][8] measured the spread factor as a function of nondimensionalized time at impact. They also presented numerical simulations to reproduce the shape of the droplet during impact for We of 90 to 800. Finally, Attane et. al. [2] constructed a second order differential equation for the energy of the system as a function of time. They developed a model to calculate the maximum spread factor and the time required to reach that maximum.

In Section 2 we present a theoretical background to the system. In Section 3 we discuss the experimental setup and data analysis. In Section 4 we present our theoretical and experimental results, and in Section 5 we present areas for future research. Finally, we summarize our findings in Section 6.

# 2 Theory

We begin by introducing a simple static model [2] for our energy balance equation, as we investigate the 2−dimensional motion of a water droplet impinging the surface of a super-hydrophobic substrate. We assume that the droplet is released from rest, and maintains azimuthal symmentry throughout the drop. This will enable us to establish the significance of some of our parameters, and to gain insight on the conservative system without dissipation. We will then incorporate the non-conservative forces to construct our time dependent model. In classical mechanics, the Hamiltonian function is

$$H = T + V \tag{1}$$

when the system is conservative, $\frac{d}{dt}H = 0$. For our model, we retain the usual translational kinetic energy, $T$ for a spherical object (in our case a water droplet), and assume that the rotational kinetic energy is negligible [4], thus

$$T = \frac{\pi}{12}\rho D_0^3 v^2 \tag{2}$$

where $\rho$ is the density of water [2]. We take the potential energy $V$ as the sum of the gravitational potential energy $E_g$ and the surface energy $E_\gamma$ [2]. Gravitational potential energy is given by

$$E_g = \frac{\pi}{6}\rho g D_0^3 h_0 \tag{3}$$

[2] at ambient temperature and pressure

where $g$ is the acceleration due to gravity, and $h_0$ is the initial height of the drop. Next, we find the surface energy using Young's Law to define the equilibrium contact angle $\theta_c$, thus

$$E_\gamma = \pi\gamma[D_0^2 - R^2\cos\theta_c] \tag{4}$$

where $R$ is the radius of the wetted area at equilibrium, and $\gamma$ the surface tension.

We now add to our model a time dependency of the following form, which allows for an understanding of the dissipation involved, and provides the basis for the system of differential equations that we create in Section 4.1

$$\frac{d}{dt}(T+V) + \Delta = 0 \tag{5}$$

Maintaining our above definitions for the kinetic and potential energies, we propose that the dissipation here is dependent upon either:

1. The initial decent, as the droplet approaches the slide with negligible surface undulations.

2. The moment of impact, while spreading or splashing occurs, until the droplet lifts (rebounds) off of the surface of the slide.

3. The rise and fall of the droplet during the first rebound. During this time, the droplet experiences observable surface deformations.

In our first case, we note that the dissipation is dominated by the drag force acting on the droplet as it falls. For a spherical fluid with Reynolds numbers ($\mathrm{Re} = \rho v D/\sigma$) in the range of $3\times10^2$ and $3\times10^5$, we define the drag force acting on our droplet to be [5]

$$F_d = \frac{\pi}{8}\rho D_0^2 c_D v^2 \tag{6}$$

where the coefficient of drag $c_D$ is a dimensionless quantity determined experimentally, and $\sigma$ is viscosity. In Section 4.1 we construct the nondimensionalized system of differential equations including this diffusion term, as well as the corresponding phase portrait. See Figure 3.

For the second case, the diffusion will be a result of the viscous fluid flow within the droplet [2], and we ignore the effects of the spreading precursor film and dissipation at the contact line due to the rapid motion of the droplet at this stage [9], [2]. The third case incorporates both the drag force and the viscous fluid flow within the droplet.

# 3 Experiment

## 3.1 Experiment Set Up

The data used in our analysis was collected from a set of videos recorded in October - November 2005 by Bojan Durickovic and Kathleen Varland, students in the University of Arizona's Program in Applied Mathematics. The videos, taken over a span of several

days, were recorded using a high speed camera[3] operated at 1000 frames per second, with a lens-to-subject length of 32 cm. The videos recorded a falling water droplet, its impact upon a substrate, and the aftermath of the collision up to near rest of the water droplet on the substrate. The only parameter that was changed in the videos was the initial height, which ranged from 1cm up to 26cm.

The camera was placed in such a way that the full impact could be viewed from the side, as well as the full rebound activity of the largest (*dominant*) water droplet to bounce after impact. Because the camera was kept a fixed distance from the substrate upon which the droplets impacted, the nozzle from which the droplet was released was only in view for the lower heights ($< 5$cm), and not all of the droplets falling trajectory was in view. The water droplets were all created using a nozzle with a tip of 1.54mm, and impacted upon a substrate that was a glass slide covered in soot/water repellent, a super-hydrophobic surface.

## 3.2 Data Analysis

As mentioned, the only variable parameter in the videos was the initial height from which the droplet was released.

| **Initial Height (cm)** | **Number of Video Samples** | **Splash on Impact** | **We Range** | **$\beta$ Range** |
|---|---|---|---|---|
| 1 | 3 | 0 | $9.6 - 10.4$ | $1.39 - 1.42$ |
| 3.3 | 2 | 0 | $30.7 - 31.4$ | $1.89 - 1.99$ |
| 5 | 3 | 0 | $47.8 - 49.9$ | $2.22 - 2.28$ |
| 6 | 3 | 0 | $61.5 - 62.3$ | $2.34 - 2.38$ |
| 6.9 | 3 | 0 | $66.1 - 73.4$ | $2.33 - 2.59$ |
| 8.5 | 3 | 0 | $87.6 - 88.7$ | $2.68 - 2.79$ |
| 9.3 | 1 | 0 | 78.1 | 2.66 |
| 10 | 2 | 1 | $83.7 - 102.5$ | $2.57 - 3.13$ |
| 10.5 | 4 | 4 | $88.2 - 110.6$ | $2.66 - 3.20$ |
| 12 | 3 | 3 | $119.6 - 127.5$ | $3.08 - 3.90$ |
| 14.5 | 2 | 2 | $152.7 - 154.3$ | $3.59 - 3.60$ |
| 15.4 | 1 | 1 | 156.2 | 4.03 |
| 26 | 3 | 3 | $278.0 - 287.1$ | $4.18 - 4.56$ |

Table 1: Video samples used for data analysis. The horizontal line at 10cm denotes the threshold at which droplets begin to splash upon impact.

Measurements were taken of each experimental sample[4], including droplet perimeter, diameter of droplet pre-impact, maximum spreading diameter of droplet upon impact, and maximum initial rebound height of droplet post-impact.

We took our measurement of the maximum spreading diameter to be the largest diameter as the droplet remained intact during impact, as viewable from the camera's viewpoint.

[3]Photron USA Fastcam X 1280 PCI 16K fps

[4]After viewing the videos in Photron Motion software, the videos were then imported into the program ImageJ for detailed analysis as image sequences.

When measuring the maximum initial rebound height, we took our measurement from the top of the substrate to the bottom of the droplet, or in the cases where the droplet had splashed on impact, we used the largest droplet. We also recorded the contact angle of the droplet at rest to be approximately $\theta_c = 140°$. Qualitatively, we also recorded whether the droplet had splashed upon impact or separated during the course of the first rebound.

# 4 Results

## 4.1 Theoretical Results

We now discuss the construction of our system of equations, and provide time dependent solutions. As noted in Section 2, we must consider three separate cases. First we discuss the initial descent. From Eqn. 5 and Eqn. 6 we have

$$\frac{d}{dt}(T+V) - F_d v = 0 \tag{7}$$

and after differentiating, we solve for the first time derivative of velocity, thus

$$\dot{v} = -g\left(1 - \frac{3c_D}{4gD_0}v^2\right) \tag{8}$$

Nondimensionalizing, we set $x = \lambda\mathcal{X}$, $v = \alpha\nu$ and $t = \beta\tau$ where $\nu, \mathcal{X}$ and $\tau$ are nondimensional. Substituting into our above equation, and setting $\dot{x} = v$ we have that

$$\mathcal{X}' = \nu \tag{9}$$
$$\nu' = 1 - \nu^2 \tag{10}$$

where $'$ denotes a single derivative with respect to $\tau$[5] . Hence we have that $\lambda = \frac{-4D_0}{3c_D}$, $\alpha = -\sqrt{-g\lambda}$ and $\beta = \sqrt{\frac{-\lambda}{g}}$. Solving the ODE in Eqn. 10 for the time dependent solution, we find that

$$\nu(t) = \frac{Ce^{2t} - 1}{Ce^{2t} + 1}. \tag{11}$$

Thus as $t \to \infty$ we see that $\nu \to 1$, which as we would expect is the characteristic terminal velocity.

Attempting to find a time-dependent solution in each of the last two cases in Section 2 is beyond the scope of this paper, and requires implementation of Navier-Stokes equations. As such, we will leave it for further research.

[5]Phase portrait created using **pplane7** http://math.rice.edu/ dfield/matlab7/pplane7.m

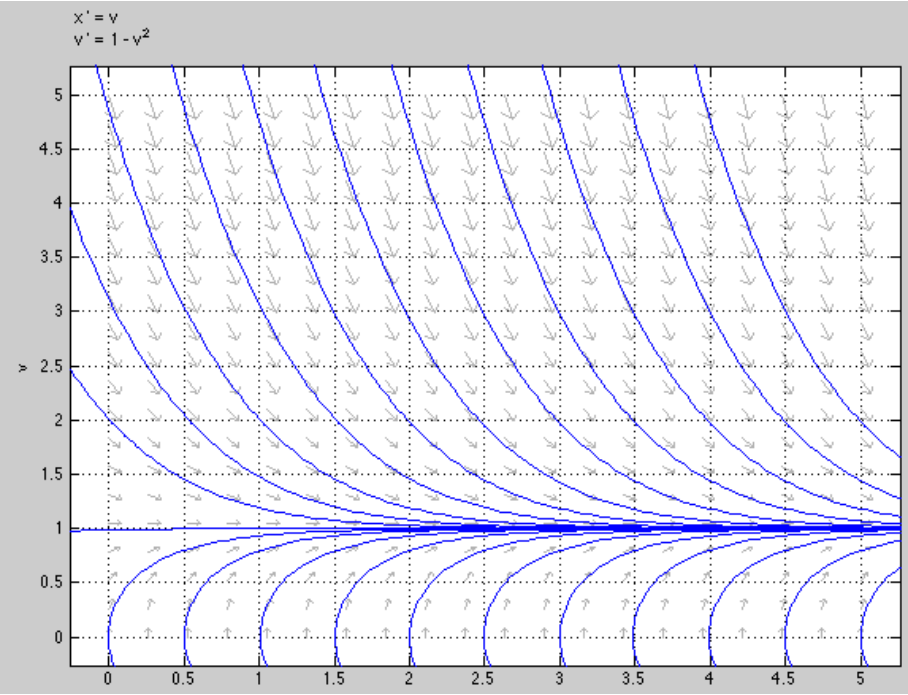


Figure 3: Phase portrait of the nondimensionalized system, Eqns. 9 & 10. Note that $\nu = 1$ represents the characteristic terminal velocity.

## 4.2 Experimental Results

With the collected data, we set out to determine the effect of both the We and spread factor $\beta$ of a droplet on its impact behavior. Specifically we investigate whether it splashed on impact or remained whole, and how high the droplet bounced on its initial rebound in relation to its initial drop height. We also examined the circularity of the droplets immediately prior to impact to determine if the droplet being oblate or prolate had an effect on its impact behavior, but found no observable relationship. In Figure 4 we see a linear relationship between the initial height, and the maximum spreading diameter ($MSD$). For those droplets that splashed on impact, we have measured the maximum spread to the the largest diameter prior to the droplet breaking apart into smaller pieces. In Figure 5 we see how the momentum of the droplet prior to impact affects its rebound height, and we clearly see different behavior between the droplets that splashed on impact, and those that remained intact.

Figure 6 shows the relationship between the spread factor $\beta$ and the coefficient of restitution $(COR) = \sqrt{h/h_0}$, where $h$ is the height of the initial rebound, and $h_0$ is the initial height. The linear fit for the droplets that did not splash on impact has a much higher slope in absolute value than the linear fit for those droplets that did splash. For those droplets that did splash, energy was lost to ejected droplets, resulting in less energy for rebound, and lower rebound height of the dominant droplet.

In Figure 7, we see a critical We number of approximately 100 which is a threshold between droplets splashing on impact or remaining intact. Although Sikalo, et. al. has

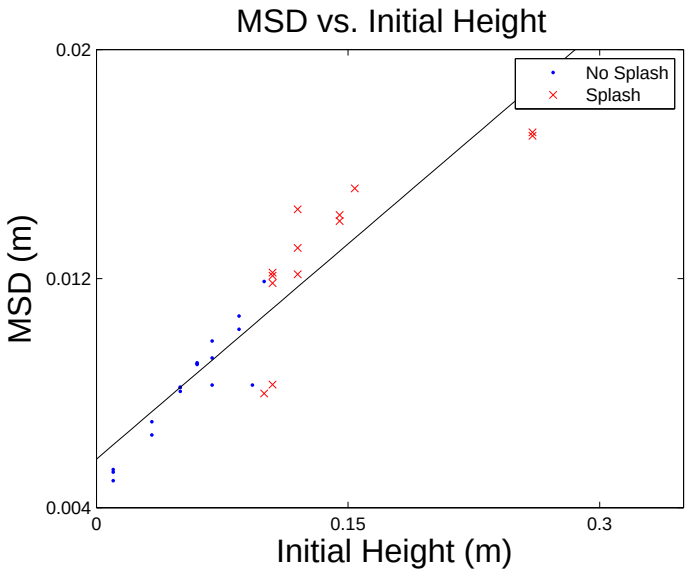


Figure 4: Effect of droplet's initial height (*velocity*) on its maximum spreading diameter upon impact. For the observed range of initial heights, the amount a droplet spreads upon impact depends linearly on its initial release height. The linear fit is $y = 0.05011x + 0.005696$. We observe there is a threshold near 10cm for which a droplet will or will not splash on impact.

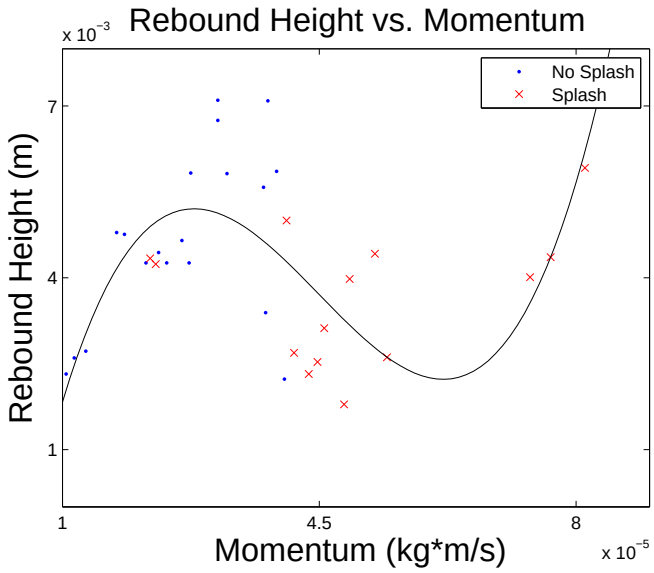


Figure 5: Effect of droplet's momentum pre-impact on its initial rebound height. We see rebound height initially increases with momentum, and drops off as there is enough momentum to cause droplets to splash upon impact. As energy is lost due to droplet splashing, the initial rebound height lessens. As momentum further increases, the energy in the system increases and rebound height again increases. The cubic fit is $y = 1.52e11x^3 - 2.05e7x^2 + 790x - 0.0042$.

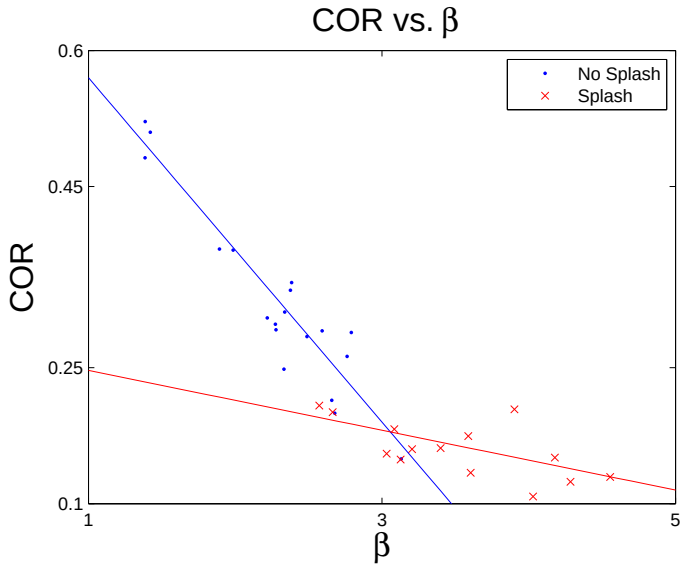


Figure 6: The effect of spread factor $\beta$ on COR (Coefficient of Restitution). The linear fit for the droplets that did not splash is $y = -0.19x + 0.76$, and the linear fit for the droplets that did splash upon impact is $y = -0.033x + 0.28$.

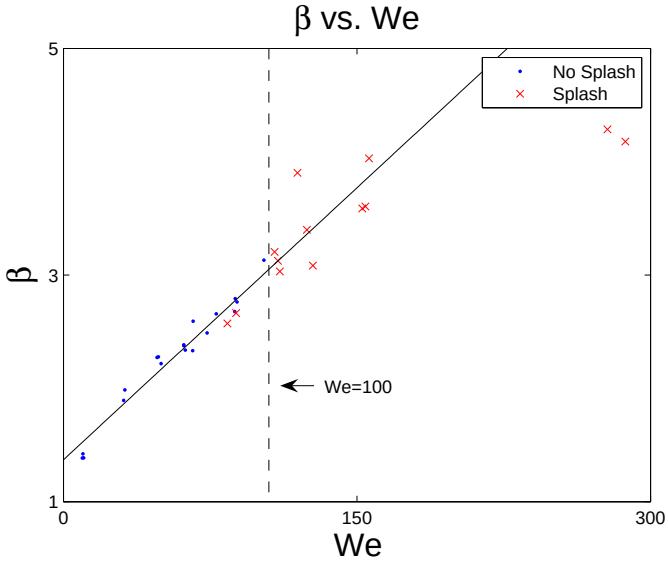


Figure 7: Effect of Weber number on spread factor $\beta$. We can see a critical Weber number of approximately 100 which will be a predictor for whether the droplet will splash upon impact. The linear data fit is $y = 0.0160x + 1.37$, and does not include the three outliers which represent the three water droplets dropped from height 26 cm.

found Weber number alone is not a sufficient predictor of this impact behavior and surface tension must also be considered [7], in our focused area of interest in a single fluid, our

experiment does not incorporate fluids of different surface tensions. Thus we may rely on the We as an accurate predictor of impact behavior.

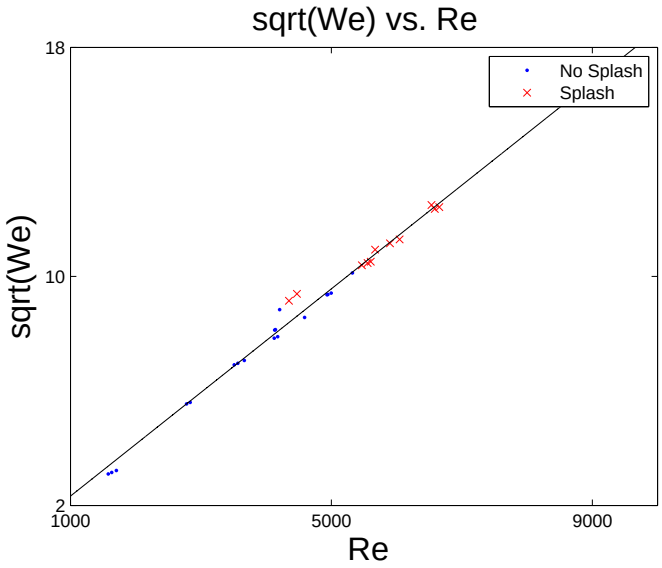


Figure 8: The slope of the linear fit $y = 0.0018x + 0.515$ is $\approx$ the Ohnesorge number of the water droplets in this We range.

In Figure 8 we plot Re (*ratio of inertial to viscous forces*) of the droplets against the square root of the We (*the ratio of inertial forces to surface tension*). The Ohnesorge number, defined to be $\text{Oh} = \sigma/(\sqrt{\gamma\rho D}) = \sqrt{\text{We}}/\text{Re}$, and is approximately the slope of the linear fit in Figure 8. From our data, for water droplets in the range $\text{We} = 30 - 150$, $\text{Oh} = 1.8 \times 10^{-3}$. For reference, the Oh of a water droplet with $\text{We} = 30$ is approximately $1.7 \times 10^{-3}$[2].

# 5 Further Research

As our data of interest was limited to video samples of just one substrate, it is necessary to examine how the droplet's impact behavior would change on other substrates of varying hydrophobicity/hydrophilicity to fully understand the behavior of the impinging water droplet. Given that our substrate surface is super-hydrophobic, with an observed contact angle of approximately $\theta_c = 140°$, we were able to effectively disregard the effect of the spreading contact line at the surface, however with more hydrophilic surfaces this dissipation effect may not be negligible [9].

Performing additional experiments at a viewpoint that would allow for analysis of the impact from above, specifically the spreading and symmetrical growth of finger formation, would also be of interest. Also, inclusion of Navier-Stokes equations into our model will allow for a better understanding of dissipation effects during impact and rebound.

# 6 Conclusions

Understanding the dynamics of water droplets is critical in many useful applications. In this paper we analyze how the We and $\beta$ of a water droplet impinging on a super-hydrophobic substrate are related to the droplet's behavior during impact and subsequent primary bounce. We derived a non-dimensional system of differential equations to model the dynamics the dissipation of energy prior to impact. Using the experimental data, we present a critical We value of 100 which is a predictor for water droplet splashing for our substrate. We also used this data to confirm the Ohnesorge number of water droplets in the We range of 30-150 to be $\approx 1.8 \times 10^{-3}$.

The authors would like to acknowledge and thank Dr. Alain Goriely and Robert Reinking for their assistance and research guidance with this paper, and the Program of Applied Mathematics at the University of Arizona.

# References

[1] Bergeron, V., Quere, D. *Water droplets make an impact.* IOP (2006).

[2] Attane, P., Girard, F. and Morin, V. *An energy balance approach of the dynamics of drop impact on a solid surface.* Phys Fluids **19** (2002).

[3] Foote, G.B. *The water drop rebound problem: Dynamics of collision.* J Atmos Sci **32** 390-402 (1974).

[4] Giancoli, D. Physics for Scientists & Engineers, Third Ed. Prentice Hall, NJ. (2000).

[5] Long, L. and Weiss, H. *The Velocity Dependence of Aerodynamic Drag: A Primer for Mathematics.* The American Mathematical Monthly, Vol. 106, No. 2 **127** (1999)

[6] Mao, T., Kuhn, D. and Tran, H. *Spread and rebound of liquid droplets upon impact on flat surfaces.* AIChE Journal **43** 2169-2179 (1997).

[7] Sikalo, S., Morengo, M., Tropea, C., & Ganic, E.N. *Analysis of impact of droplets on horizontal surfaces.* Exp Therm Fluid Sci **25** 503-510 (2001).

[8] Sikalo, S., Ganic, E.N. *Phenomena of droplet-surface interactions.* Exp Therm Fluid Sci **31** 97-110 (2006).

[9] Xu, H., Shirvanyants, D., Beers, K., Matyjaszewski, K., Rubinstein, M., Sheiko, S. *Molecular motion in a spreading precursor film.* Phys Rev Lett **93** 206103 (2004).